Contents lists available at ScienceDirect

Landscape and Urban Planning

Research Paper

Impact of urban form and design on mid-afternoon microclimate in Phoenix Local Climate Zones

Ariane Middel [a,*], Kathrin Häb [b], Anthony J. Brazel [c], Chris A. Martin [d], Subhrajit Guhathakurta [e]

[a] Center for Integrated Solutions to Climate Challenges, Arizona State University, United States
[b] Department of Computer Science, University of Kaiserslautern, Germany
[c] School of Geographical Sciences and Urban Planning, Arizona State University, United States
[d] Science and Mathematics Faculty, School of Letters and Sciences, Arizona State University, United States
[e] Center for Geographic Information Systems, Georgia Institute of Technology, United States

HIGHLIGHTS

- Cooling is not only a function of vegetation and surface materials, but also dependent on the form and spatial arrangement of urban features.
- At the microscale, urban form has a larger impact on daytime temperatures than landscaping.
- In mid-afternoon, dense urban forms can create local cool islands.
- Spatial differences in cooling are strongly related to solar radiation and local shading patterns.
- The LCZ classification scheme is a useful concept for integrating local climate knowledge into urban planning and design practices.

ARTICLE INFO

ABSTRACT

This study investigates the impact of urban form and landscaping type on the mid-afternoon microclimate in semi-arid Phoenix, Arizona. The goal is to find effective urban form and design strategies to ameliorate temperatures during the summer months. We simulated near-ground air temperatures for typical residential neighborhoods in Phoenix using the three-dimensional microclimate model ENVI-met. The model was validated using weather observations from the North Desert Village (NDV) landscape experiment, located on the Arizona State University's Polytechnic campus. The NDV is an ideal site to determine the model's input parameters, since it is a controlled environment recreating three prevailing residential landscape types in the Phoenix metropolitan area (mesic, oasis, and xeric). After validation, we designed five neighborhoods with different urban forms that represent a realistic cross-section of typical residential neighborhoods in Phoenix. The scenarios follow the Local Climate Zone (LCZ) classification scheme after Stewart and Oke. We then combined the neighborhoods with three landscape designs and, using ENVI-met, simulated microclimate conditions for these neighborhoods for a typical summer day. Results were analyzed in terms of mid-afternoon air temperature distribution and variation, ventilation, surface temperatures, and shading. Findings show that advection is important for the distribution of within-design temperatures and that spatial differences in cooling are strongly related to solar radiation and local shading patterns. In mid-afternoon, dense urban forms can create local cool islands. Our approach suggests that the LCZ concept is useful for planning and design purposes.

© 2013 The Authors. Published by Elsevier B.V. Open access under CC BY-NC-SA license.

* Corresponding author at: Center for Integrated Solutions to Climate Challenges, Arizona State University, PO Box 878009, Tempe, AZ 85287-8009, United States. Tel.: +1 480 414 6793.
E-mail addresses: ariane.middel@asu.edu (A. Middel), kathrin.haeb@cs.uni-kl.de (K. Häb), abrazel@asu.edu (A.J. Brazel), Chris.Martin@asu.edu (C.A. Martin), subhro.guha@coa.gatech.edu (S. Guhathakurta).

1. Introduction

Urban heat island (UHI) effects, induced by anthropogenic changes in land cover and built forms, have been studied extensively in cities around the world (Arnfield, 2003). In desert environments, where daytime temperatures and solar intensity are high, local climate modifications through heat islands put additional stress on the urban ecosystem. These increased temperatures have implications for outdoor water use, air quality, and energy use for air conditioning, thus adversely affecting human well-being (Golden, 2004; Guhathakurta & Gober, 2007; Harlan, Brazel, Prashad, Stefanov, & Larsen, 2006; Sarrat, Lemonsu, Masson, & Guedalia, 2006). Knowledge of mitigating UHI effects has grown steadily during the last two decades. One method of ameliorating daytime and nighttime temperatures is to increase the amount of vegetation, providing cooling through shading and evapotranspiration. In desert cities, where water resources are scarce, this approach creates a cooling-water use tradeoff that needs to be optimized to find a sustainable balance between temperature reduction achieved and the amount of water used (Gober et al., 2012; Middel, Brazel, Gober, et al., 2012; Middel, Brazel, Kaplan, & Myint, 2012; Shashua-Bar, Pearlmutter, & Erell, 2009). However, the most sustainable solution may not be the best from a human vulnerability standpoint (Jenerette, Harlan, Stefanov, & Martin, 2011; Middel, Brazel, Kaplan, et al., 2012). Other studies have explored reducing high heat resulting from the UHI through comprehensive neighborhood and urban design, particularly in semi-arid regions. A recent study by Guhathakurta and Gober (2010) confirmed that the type and arrangement of vegetation significantly influence microclimatic variations. Other efforts found that land use, density, and residential parcel design impact UHIs and microclimate (Bonan, 2000; Hart & Sailor, 2009; Stone & Norman, 2006). Pearlmutter, Krüger, and Berliner (2009) developed a metric called "complete vegetated fraction", which allows for studying the three-dimensional urban surface geometry and vegetation in an integrated form. They found that the latent heat flux almost linearly increased with the vegetation fraction and was offset by a decrease in heat storage and sensible heat flux.

Natural desert environments are usually characterized by large diurnal temperature differences, low humidity, and strong winds, and therefore have great potential for UHI mitigation through urban form and design (Pearlmutter, Berliner, & Shaviv, 2007b). Emmanuel and Fernando (2007) found that urban morphology significantly affects daytime air temperatures. High density urban areas provide shading from incoming solar radiation and can therefore result in cooling benefits. This is known as a "cool island" effect (Pearlmutter, Bitan, & Berliner, 1999), and is primarily a daytime phenomenon (Brazel, Selover, Vose, & Heisler, 2000; Georgescu, Moustaoui, Mahalov, & Dudhia, 2011).

In this study, we systematically analyze the daytime microclimate of typical Phoenix neighborhood types—xeric, mesic and oasis—to evaluate their cooling and warming potential related to landscaping and the built environment. The goal is to find the most effective urban form and design strategies across a range of Phoenix urban forms, classified into Local Climate Zones (LCZs), to ameliorate mid-afternoon temperatures during the summer. Our results provide insight into the impact of urban form and design on microclimate in desert environments and showcase the utility of the LCZ concept for urban planning and design purposes.

2. Methods

We simulated micro-scale thermal interactions with ENVI-met Version 3.1 BETA V (Bruse, 2013) to investigate effects of urban form and landscaping on mid-afternoon microclimate in five representative neighborhoods of the Phoenix metropolitan area. ENVI-met is a three-dimensional (3D) Computational Fluid Dynamics model that simulates surface–plant–air-interactions in urban environments. Buildings, vegetation, and surfaces in the area of interest are designed on a 3D grid at a typical resolution of 0.5–10 m. The ENVI-met core uses a full 3D prognostic meteorological model to calculate main wind flow, temperature, humidity, and turbulence (Bruse, 2004). It is coupled with a 1D model that extends up to 2500 m above ground level to simulate processes at the boundary layer. ENVI-met further incorporates a simple 1D soil model (3D for the first grid layer below the surface) that calculates the heat transfer between the surface and the ground, soil temperature, and soil water content up to 2-m depth.

ENVI-met simulations typically cover 24–48 h and result in atmospheric outputs for each grid cell in the 3D raster as well as surface and soil variables for the simulated environment. In addition, receptors can be placed in the model domain to record atmospheric conditions at a user-specified location. Selected output variables include longwave and shortwave radiation; air, surface, and wall temperatures; latent and sensible heat fluxes; and Predicted Mean Vote (PMV), an indicator of thermal comfort.

ENVI-met was originally developed in Germany for temperate climate zones, but has been successfully applied to Phoenix in several studies (Chow & Brazel, 2011; Chow, Pope, Martin, & Brazel, 2011; Emmanuel & Fernando, 2007). To validate our simulation for desert environments, we adjusted certain model parameters, e.g., variables related to vegetation characteristics. We assessed the accuracy of the ENVI-met model by comparing observed temperatures to modeled temperatures in three adjacent experimental residential neighborhoods. We ran ENVI-met for June 23, 2011, a typical summer day with low temperatures of 26 °C at 04:00 h and high temperatures of 43 °C at 16:00 h, no precipitation, and no cloud cover (MesoWest, 2012).

Following the model validation, we designed thirteen combined urban form and landscaping scenarios that correspond to existing neighborhoods in the Phoenix metropolitan area. We simulated diurnal daytime microclimatic conditions in ENVI-met using the parameters determined in the validation process and conducted a micro-level analysis of urban form and landscape design impacts on 2-m air temperatures (T_{2m}). We investigated diurnal temperature variations, the spatial temperature distribution at mid-afternoon (15:00 h), ventilation, and shading in each combined scenario. We also examined the relationship of surface temperatures to surface materials and incoming solar radiation for a high-density, low-water-use vegetation scenario.

2.1. Study site

The North Desert Village (NDV) residential community at Arizona State University's Polytechnic campus was selected as the study site for this project. The NDV is a neighborhood-scale landscape design experiment that was established in 2005 to study human–landscape interactions and explore the impact of residential landscape design on urban ecosystems (Martin, Busse, & Yabiku, 2007). Three mini-neighborhoods (blocks of six households each) in the 152 single-family home community were designed to represent typical residential yardscape types in the Phoenix metropolitan area, i.e., mesic, oasis, and xeric landscaping (Fig. 1). Mesic landscaping comprises a mix of non-native, high water-use plants, shade trees, and expansive turf grass, all of which are irrigated by an above ground sprinkler system. Oasis landscaping combines drip-irrigated, high and low water-use plants in decomposing granite mulch (5-cm depth) with patches of sprinkler-irrigated turf grass. Xeric sites include drip-irrigated, low water-use native and/or desert-adapted plants in decomposing granite mulch.
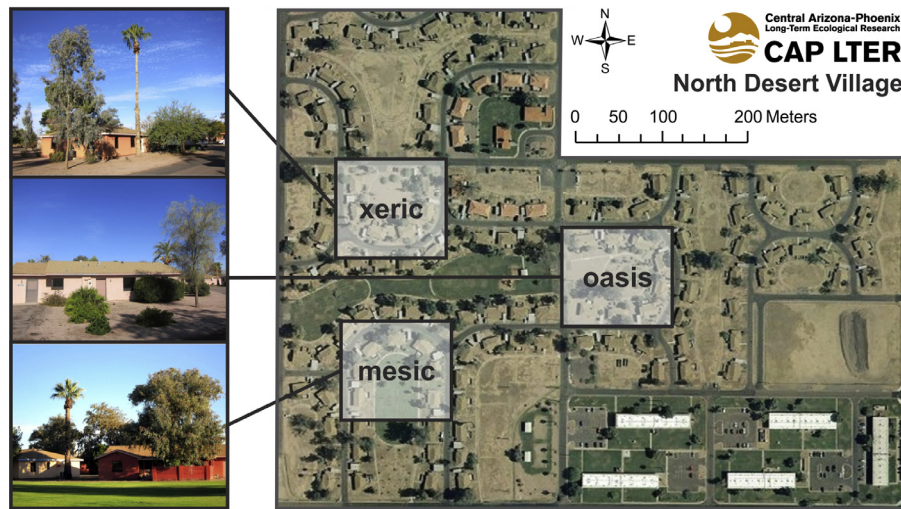
Fig. 1. North Desert Village experimental suburb in Phoenix, AZ, with four prevailing residential neighborhood landscape types.

Micrometeorological stations installed in the center of each mini-neighborhood continuously monitor soil and atmospheric conditions for each of the three sites. In addition, outdoor water use for landscape irrigation in each mini-neighborhood is recorded monthly. These data allow us to parameterize and evaluate the ENVI-met model by comparing the NDV microclimate observations to the simulated microclimate data. The mini-neighborhoods are 115–120 m in length, and therefore smaller than the estimated flux footprint of 200 m of a typical 2-m weather station. We acknowledge that the source area of the observation is larger than the model domain. To our knowledge, however, the NDV is the only controlled landscaping experiment in the Phoenix metropolitan area that allows us to conduct our study. The NDV observations are biased toward the surrounding uncontrolled landscapes, thereby reducing the impacts related to the mesic-oasis-xeric maximum temperature progression. Regardless, these effects are estimated to be smaller than the air temperature sensor accuracy of 0.3–0.5 °C.

2.2. Data

The ENVI-met model requires a vegetation database, physical soil structure and profile information, and two user-defined text-based input files. The so-called area input file (*.in) is a 3D representation of the modeled scene that defines the arrangement of built structures, surface characteristics, and vegetation. A configuration file (*.cf) contains meteorological data to initialize the model parameters for the date of simulation. Required data include air and soil temperature, relative humidity, wind speed and direction, and soil moisture. Incoming solar radiation is calculated by ENVI-met based on latitude/longitude, date, time, and cloud cover. The following sections detail data requirements for each input and our acquisition method for the necessary parameters to run ENVI-met.

2.2.1. Weather data

We obtained hourly temperature, humidity, and wind data for June 23, 2011 from three different sources. Hourly air, surface, and soil temperatures were retrieved from the fixed solar-powered micrometeorological stations near the center of each NDV study area. At each station, air temperatures (2-m height) were recorded with shielded copper constantan thermocouples. Surface temperatures were recorded by IRR-PN infrared radiometer sensors (www.apogeeinstruments.com) mounted at 2-m height at a 45° angle perpendicular to the surface. The sensor angle of view was 18°. The IRR accuracy is 0.2 °C at 95% confidence. Soil temperatures

(30-cm depth) were recorded using a pair of copper constantan thermocouples at each site. The soil thermocouples at the oasis site were positioned under both turf and decomposing granite surface covers. The air and soil temperature thermocouple wires were tested for accuracy prior to their installation at NDV. The range of accuracy was between 0.3° and 0.5 °C. All sensors recorded data every 5 min. Data were averaged hourly by a CR1000 datalogger (www.campbellsci.com). Specific humidity values were obtained at 2500 m for Phoenix from the University of Wyoming (2013) Department of Atmospheric Sciences. Wind speed data at 10 m above ground along with data for the most frequent diurnal wind direction, cloud cover, and relative humidity at 2-m height were acquired from the MesoWest Phoenix-Mesa Gateway weather station (MesoWest, 2012). This station is located 2.5 km east of the study area next to the Phoenix-Mesa Gateway Airport.

2.2.2. Vegetation data

The vegetation parameters required by ENVI-met for the NDV simulation were collected on-site. An initial analysis of all existing vegetation resulted in the identification of four vegetation types—lawns, small succulents, trees, and shrubs. Lawns in the mesic and oasis study area were modeled as Bermuda grass (*Cynodon dactylon*), a typical heat- and drought-resistant summer grass in Phoenix. Small succulents (diameter < 1 m and therefore smaller than a grid cell) in the xeric and oasis study areas were omitted under the assumption that they do not significantly influence microclimate through evapotranspiration or shading. Finally, we created a complete inventory of trees and shrubs for each of the three study areas, including species name, observed height, canopy volume, and location.

For trees that were at full leaf during our field measurements, we determined the normalized vegetation leaf area density (LAD) with a LI-COR® LAI-2000 Plant Canopy Analyzer under cloudy conditions. The LAD values for all other trees were estimated using a regression model by Jenkins, Chojnacky, Heath, and Birdsey (2004). This model renders a leaf area index (LAI) value for hardwood and softwood trees by multiplying the specific leaf area of a tree with the estimated total foliage biomass based on the tree diameter at breast height (1.3 m above ground). In a second step, the maximum LAD value and its vertical distribution in 10 different heights, as required by ENVI-met, was calculated after Lalic and Mihailovic (2004). The root depth for all trees was estimated using a regression model developed by Schenk and Jackson (2002). Altogether,

Table 1

Perennial trees, shrubs, and vines present (•) in the NDV study area; species name and occurrence (M = mesic, O = oasis, X = xeric).

Trees	M	O	X	Shrubs and vines	M	O	X
Acacia salinica		•		*Bougainvillea hybrid*		•	
Acacia stenophylla	•	•	•	*Caesalpinia pulcherrima*		•	
Brachychiton populneus	•		•	*Caesalpinia gilliesii*			•
Brahea armata			•	*Calliandra californica*			•
Corymbia papuana		•		*Carissa macrocarpa*		•	
Eucalyptus camaldulensis	•	•		*Chamaerops humilis*		•	
Eucalyptus microtheca			•	*Encelia farinosa*			•
Eucalyptus polyanthemos	•			*Hesperaloe parviflora*			•
Fraxinus uhdei		•		*Lantana hybrid*		•	
Fraxinus velutina			•	*Leucophyllum candidum*			•
Malus (apple)	•			*Leucophyllum frutescens*		•	
Melaleuca viminalis			•	*MacFadyena unguis-cati*		•	
Myrtus communis	•	•		*Myrtus communis*	•	•	
Parkinsonia hybrid			•	*Nerium oleander*		•	•
Phoenix dactylifera		•	•	*Rosa hybrid*	•		
Pinus eldarica	•	•		*Ruellia brittoniana*		•	
Pinus halepensis			•	*Ruellia peninsularis*			•
Pistacia chinensis	•			*Tecoma capensis*	•		•
Platanus wrightii	•						
Platycladus orientalis	•	•	•				
Prosopis hybrid			•				
Prunus cerasifera		•					
Ulmus parvifolia	•	•					
Washingtonia filifera			•				

the study sites encompassed 233 shrubs and 126 trees at the time of observation (for a list of species, see Table 1).

2.2.3. Soil data

The prevalent soil for the study sites is Mohall loam (NRCS, 2012), which consists of loam, clay loam, and sandy clay loam (Adams, 1974). The parameters for these soil types are part of the default ENVI-met soils database. In the xeric and oasis neighborhoods, all non-grass surfaces are covered with a 5 cm layer inorganic mulch (decomposing granite). Mulch is often used for desert landscaping in the southwestern United States to lower maintenance and to reduce soil evaporation rates. The physical characteristics of decomposing granite were retrieved from Singer and Martin (2008). As an estimate for the initial below ground soil temperature, we used observations from the NDV sensors that continuously record soil temperatures near the center of each study area. In addition, NDV volumetric water content observations at 30 cm depth were retrieved to determine initial soil moisture values for each study area.

2.2.4. Building data

The current ENVI-met model (V. 3.1 BETA V) only supports uniform building materials for all structures in a simulation. The NDV study sites feature detached 1-story single family homes with similar floor plans and identical building materials, i.e. stucco walls and asphalt shingle roofs. For the simulation, we retrieved thermophysical properties from the Fraunhofer IRB (2012) materials data base. Interior temperatures for the buildings were set to 20 °C.

2.3. ENVI-met model evaluation

To create a digital representation of the validation sites and set up the ENVI-met area input files, we digitized buildings and surfaces of the three NDV neighborhoods in ESRI's ArcGIS 10 from the Bing Maps Aerial layer (Fig. 2). Vegetation was geocoded from the field-based plant inventory. From the ArcGIS shape files, we produced 3D area input files in ENVI-met with a grid resolution of 1 m, resulting in area input files of $115 \times 115 \times 30$ grids (mesic), $120 \times 120 \times 30$ grids (oasis), and $115 \times 100 \times 30$ grids (xeric). Finally, we added three nesting grids on each side, which increased the numerical stability of the simulation with objects

close to the border of the study area. A receptor (weather logger) was placed at the location of the weather station in each of the three input area files for comparison of measured and modeled microclimatic conditions (Fig. 2).

We ran ENVI-met for a 45 h period, starting at 03:00 h, with constant time steps (2 s) and model output every 60 min, using the configuration parameters described in Section 2.2 and listed in Table 2. We discarded the first 22 h of the model run, because the ENVI-met model requires spin-up time. This approach doubles the model-run time, but increases the overall performance of the model, especially in the afternoon and evening hours.

Hourly air temperature data observed at the NDV weather stations were compared to modeled temperatures at the receptor location in each study area. In addition, modeled surface temperatures in the xeric study area were validated using the data recorded by the infrared radiometer sensors. Simulated and observed air temperatures showed very good agreement in the morning, but observed temperatures were underestimated by ENVI-met in the afternoon.

As expected, the mesic site was coolest by 1 °C or more compared to the other sites. Modeled and measured temperature maximums in this study area were 43.4 °C and 42.3 °C, respectively. The xeric site was the hottest mini-neighborhood with temperatures peaking at 44.8 °C (modeled) and 44.4 °C (observed). Surface temperatures at the receptor location in the xeric area refer to inorganic mulch and are overestimated by ENVI-met in the morning with a better fit in the afternoon and at night.

To evaluate the accuracy of our validation, we followed the methodology suggested by Willmott (1981, 1982) calculating the root mean square error (RMSE) and the index of agreement (d). The RMSE provides insight into the general model performance by measuring the average difference between observed (O) and modeled (P) values, in our case, T_{2m}. The error is further split into a systematic and unsystematic component. The systematic RMSE measures the error introduced by the model design or systematic errors in the initialization values of the model or the observations and should be minimized, while the unsystematic error should approach the overall RMSE. The index of agreement d, ranging from 0.0 to 1.0, is a descriptive measure for model evaluation and measures the degree to which the modeled values are error free, with $d = 1.0$ indicating that P equals O (Willmott, 1981).

Fig. 2. Base maps of the ENVI-met area input files for the four North Desert Village treatment areas, including buildings, surfaces, vegetation, and weather station.

The agreement between measured and simulated 2-m air temperatures is very good for all validation runs (Fig. 3 and Table 3). The index d ranges from 0.97 (xeric) to 0.99 (mesic), indicating that our ENVI-met simulations capture the observed diurnal temperature trends well. The xeric study area holds the lowest d (0.97) and the largest RMSE (overall: 2.0 °C; systematic: 1.62 °C; unsystematic: 3.42 °C) of all of the sites.

For the oasis neighborhood, ENVI-met overestimates 2-m air temperatures in the early morning to mid-afternoon and underestimates temperatures from mid-afternoon to midnight. In the xeric study area, the model underestimates late-afternoon air temperatures while overestimating temperatures in the early morning and at night. Our simulations only slightly overestimate daily peak temperatures, as opposed to other studies validating ENVI-met for

Table 2
ENVI-met parameters as specified in the configuration file for the four NDV study areas.

ENVI-met input parameters		Mesic	Oasis	Xeric
Soil data				
Initial temperature, upper layer (0–20 cm)	[K]	299.62	306.4	306.55
Initial temperature, middle layer (20–50 cm)	[K]	300.62	307.4	307.55
Initial temperature, deep layer (>50 cm)	[K]	301.62	308.4	308.55
Relative humidity, upper layer (0–20 cm)	[%]	35.00	25.00	15.00
Relative humidity, middle layer (20–50 cm)	[%]	40.00	30.00	20.00
Relative humidity, deep layer (>50 cm)	[%]	45.00	35.00	25.00
Building data		All treatments		
Inside temperature	[K]	293.00		
Heat transmission walls	[W m^{-2} K]	1.60		
Heat transmission roofs	[W m^{-2} K]	6.00		
Albedo walls	[–]	0.55		
Albedo roofs	[–]	0.20		
Meteorological data				
Wind speed, 10 m above ground	[m s^{-1}]	1.50		
Wind direction (0:N, 90:E, 180:S, 270:W)	[°]	280		
Roughness length at reference point	[m]	0.01		
Initial temperature atmosphere	[K]	299.00		
Specific humidity in 2500 m [water/air]	[g kg^{-1}]	2.39		
Relative humidity in 2 m	[%]	23.00		
Cloud cover	[x/8]	0.00		

Table 3
Evaluation of model performance (MBE: mean bias error; RMSE: root mean square error; MAE: mean absolute error; d: index of agreement; MSE: mean square error).

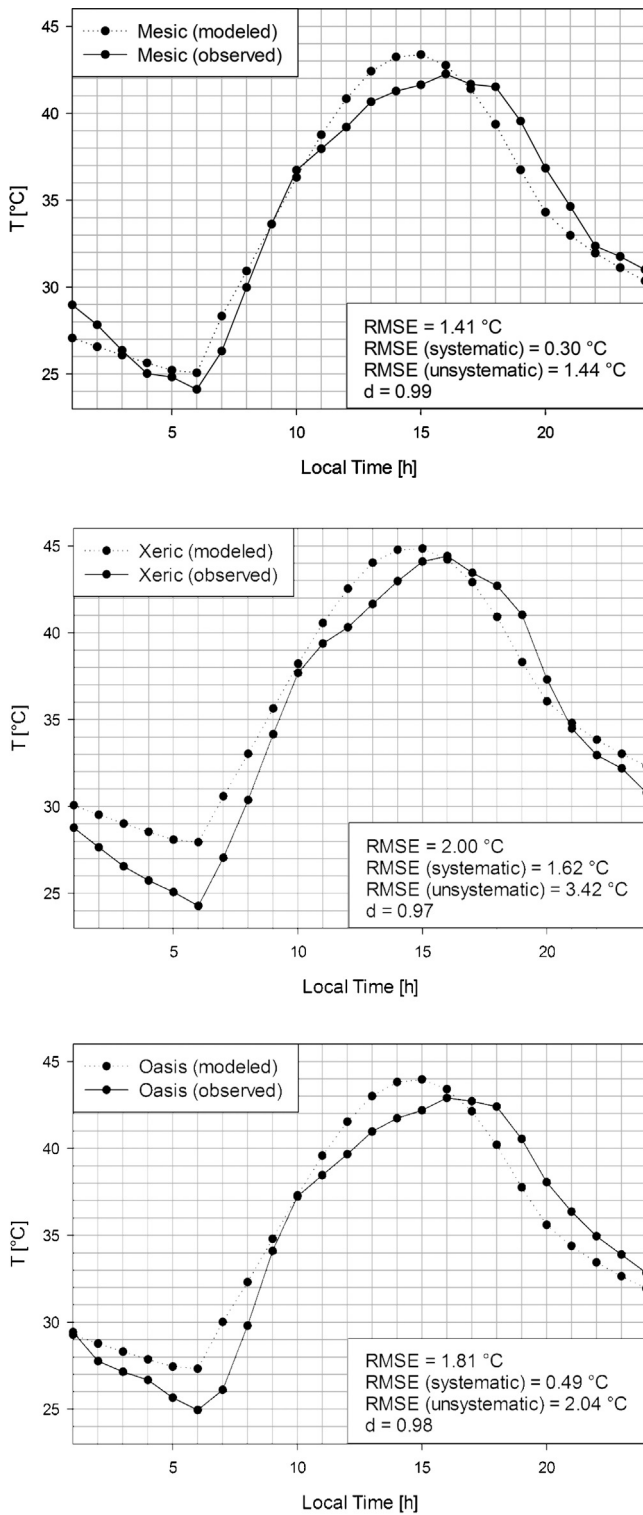|	Air temperature at 2 m [°C]			Surface temperature [°C]
	Mesic	Oasis	Xeric	Xeric
MBE	−0.02	0.43	1.20	1.89
RMSE	1.41	1.81	2.00	3.17
MAE	1.18	1.58	1.74	2.73
d	0.99	0.98	0.97	0.97
MSE systematic	0.09	0.24	2.62	4.51
MSE unsystematic	2.07	4.17	11.71	23.78
RMSE systematic	0.30	0.49	1.62	2.12
RMSE unsystematic	1.44	2.04	3.42	4.88

Fig. 3. Validation results for June 23, 2011: diurnal hourly 2-m air temperatures (modeled vs. observed) for xeric, oasis, and mesic.

Fig. 4. Diurnal wind direction profile for June 23, 2011 (MesoWest, 2012).

the Phoenix metropolitan area. Emmanuel and Fernando (2007) reported an overestimation of 2-m air temperatures for downtown Phoenix after midnight and in the morning. Their model run underestimated temperatures from afternoon to midnight. Chow and Brazel (2011) presented an ENVI-met validation that generally underestimates daytime 2-m air temperatures, but overestimates nighttime temperatures. A graph comparing simulated and measured air temperatures at 2-m height in Chow and Brazel (2011)
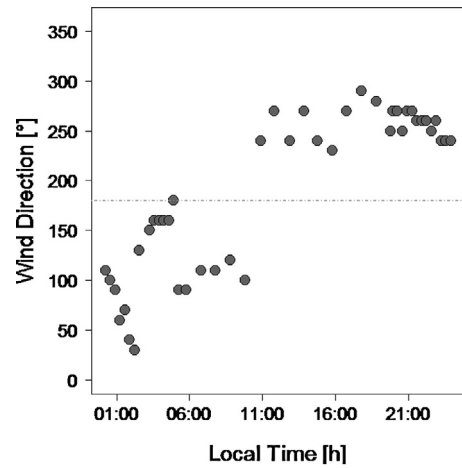
shows a similar trend, but slightly shifted. Here, the model overestimates air temperatures in the late afternoon and at night.

A noticeable difference between modeled and observed 2-m air temperatures is a phase shift between the temperatures. The diurnal maximum is brought forward by up to an hour in the simulations. This trend can also be observed in the model validations presented by Chow and Brazel (2011) and Emmanuel and Fernando (2007). Both the phase shift and the underestimation of observed temperatures during the day and the overestimation during the night can be attributed to the inadequate computation of heat storage in ENVI-met, as it was also reported by the above cited studies. ENVI-met is not able to simulate the heat storage of buildings, since each house is given the same initial indoor temperature, which is kept constant during the simulation. Furthermore, the soil model in ENVI-met is only one-dimensional, i.e., it does not incorporate horizontal heat transfer within the ground.

The shifted maximum air temperature might also be further influenced by a mesoscale thermodynamic circulation which is common for the Phoenix metropolitan area as shown in previous studies (Balling & Cerveny, 1987; Ellis, Hildebrandt, Thomas, & Fernando, 2000). Ellis et al. (2000) found that wind speeds on high ozone days in Phoenix are low and that the predominant wind veers from southerly-southeasterly in the morning to westerly-southwesterly in the afternoon and evening. Balling and Cerveny (1987) investigated long-term associations between wind and the urban heat island in Phoenix and showed that winds are directly related to the development of a pronounced heat island. Fig. 4 maps the diurnal wind direction recorded at the MesoWest weather station near the NDV sites for June 23, 2011, revealing a change in wind direction at around 11:00 h. ENVI-met is not capable of incorporating veering winds; both wind speed and direction are initialized through the configuration file and remain stable throughout the simulation. Therefore, thermal wind systems that warm or cool the atmosphere cannot be taken into account.

The index of agreement d for modeled surface temperatures in the xeric study area is 0.97 (Fig. 5), but the $RMSE$ is higher than for the diurnal 2-m air temperature simulation (3.17 °C vs. 2.00 °C). Since the weather station in the xeric area is set up on inorganic mulch, the observed data are not suitable to validate surface temperatures for other surface types in this study area, i.e. asphalt and concrete. In an attempt to get an estimate for impervious surfaces, we mapped the surface temperatures for 15:00 h and visually compared asphalt and concrete temperatures to observations we made on June 18, 2013 for an ongoing tree and shade study. The weather on June 18, 2013 was very similar to June 23, 2011 with a temperature maximum of 42.8 °C at 16:00 h and no cloud cover.
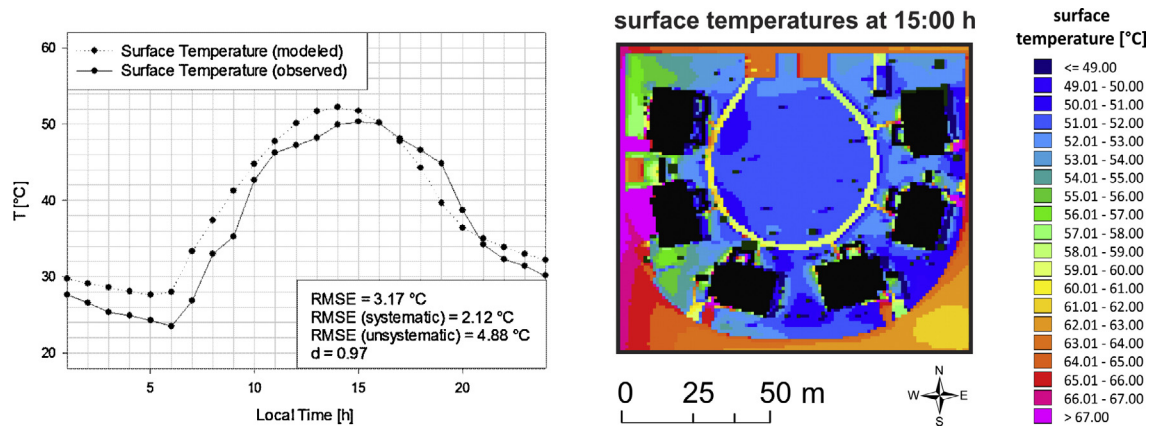
Fig. 5. Diurnal surface temperatures (modeled vs. observed) for the xeric validation site (left); spatial plot of surface temperatures at 15:00 h (right).

At 15:00 h, air temperature differences between these two days were 0.6 °C. As part of the tree and shade study, we sampled surface temperatures of six sun exposed asphalt and concrete surfaces in a Phoenix metropolitan area neighborhood called Power Ranch at 15:00 h with an infrared radiometer sensor mounted to a golf cart. Observations yielded an average temperature of 64.6 °C for asphalt and 56.7 °C for concrete. These measurements are in good agreement with the surface temperatures modeled with ENVI-met (62 °C–65 °C for asphalt, 57 °C–60 °C for concrete, Fig. 5, right).

In conclusion, our validation parameters are considered adequate for the microscale simulation of the different neighborhoods. Overall, the thermal hierarchy of the three neighborhoods is captured well in the simulations. Mesic is modeled and observed as the coolest study area followed by the oasis neighborhood and the xeric site. The present agreement between model and observations is surprisingly good and better than in most other studies due to a longer spin-up time and refined model parameters for soil and vegetation.

2.4. Urban form and landscaping scenarios

The Phoenix metropolitan area mainly features low-density urban developments with wide streets, a high percentage of single-family detached homes, and some lowrise apartments. For this study, we chose five neighborhoods that portray a cross-section of typical residential neighborhoods in the Phoenix metropolitan area (Fig. 6). We combined these neighborhoods with mesic, oasis, and xeric landscape designs to create distinct urban form and landscaping scenarios. We classified the urban forms into Local Climate Zones (LCZ), a classification system developed by Stewart and Oke (2012) to report urban climate findings in a standardized fashion. LCZs are regions of 10^2 m to 10^4 m length that are differentiated by urban form and surface properties, e.g., impervious fraction, and building height and spacing (Table 4).

Each zone is characterized by a uniform surface–air temperature distribution under calm, clear conditions, and therefore exhibits a typical local climate. From the hierarchy of 16 LCZs defined in the urban–rural transect (Stewart & Oke, 2012), our neighborhoods represent the zones: *Open Lowrise*, *Open Midrise*, *Compact Lowrise*, *Compact Midrise*, and *Compact Highrise*. To model the *Open Lowrise* urban form and landscaping scenarios, we selected a neighborhood in Mesa, Arizona, with 28 uniformly arranged detached 2-story homes. These buildings are surrounded mostly by pervious surfaces, but have road access with minimal setback from the street. For the second set of scenarios, *Open Midrise*, we chose a condominium community in Scottsdale, Arizona, with five large, widely set 7-story buildings. The multi-unit condominiums are surrounded by pervious ground and connected to the main street through small paths.

The *Compact Lowrise* scenarios were created from a high-density neighborhood in Mesa. This setting includes 46 small, detached 2-story single-family homes that are surrounded only by little pervious surfaces and arranged in a grid pattern along narrow residential streets. In contrast, the *Compact Midrise* scenarios include close-set 3-story apartments near Phoenix downtown with inner courtyard and surrounding access roads. Finally, the *Compact Highrise* scenario represents a block in downtown Phoenix with a dense mix of close-set high-rise buildings of steel, concrete, and glass. The buildings are surrounded by major roads, little or no pervious surfaces, and the sky view factor is significantly reduced.

Combining the low- and midrise urban forms with the three landscape designs, we kept the amount of trees, shrubs, and grass per square meter constant to match the amount of vegetation at the validation sites. The *Compact Highrise* neighborhood was not combined with different landscaping options due to a lack of pervious surfaces and designed with few xeric trees and shrubs. Soil and atmospheric parameters for the combined scenarios were adopted from the validation runs. To account for building materials in the midrise and highrise scenarios, we adapted building parameters from the Fraunhofer IRB (2012) materials data base for the dominant materials used in these scenarios. Building materials for the lowrise scenarios were chosen to be the same as in the validation runs.

3. Results

In the following discussion, we focus our analysis on the spatial distribution and variation of 2-m air temperatures T_{2m} and the relationship between surface temperatures, short-wave radiation, and surface materials. We particularly focus on mid-afternoon microclimate, i.e., 15:00 h on June 23, 2012, the time of maximum thermal stress for pedestrians.

3.1. Diurnal air temperature variation

We calculated the hourly spatial average of near-ground air temperatures T_{2m} in each grid cell (excluding buildings) and the respective standard deviation for each of the 13 scenarios to investigate the diurnal temperature variation (Fig. 7). The standard deviation, also shown in Fig. 7, was used as a measure for the spatial variability of T_{2m}. As temperatures increase, variability increases with maximum values at 15:00 h. The compact scenarios exhibit larger variability than their open equivalents. The highrise scenario
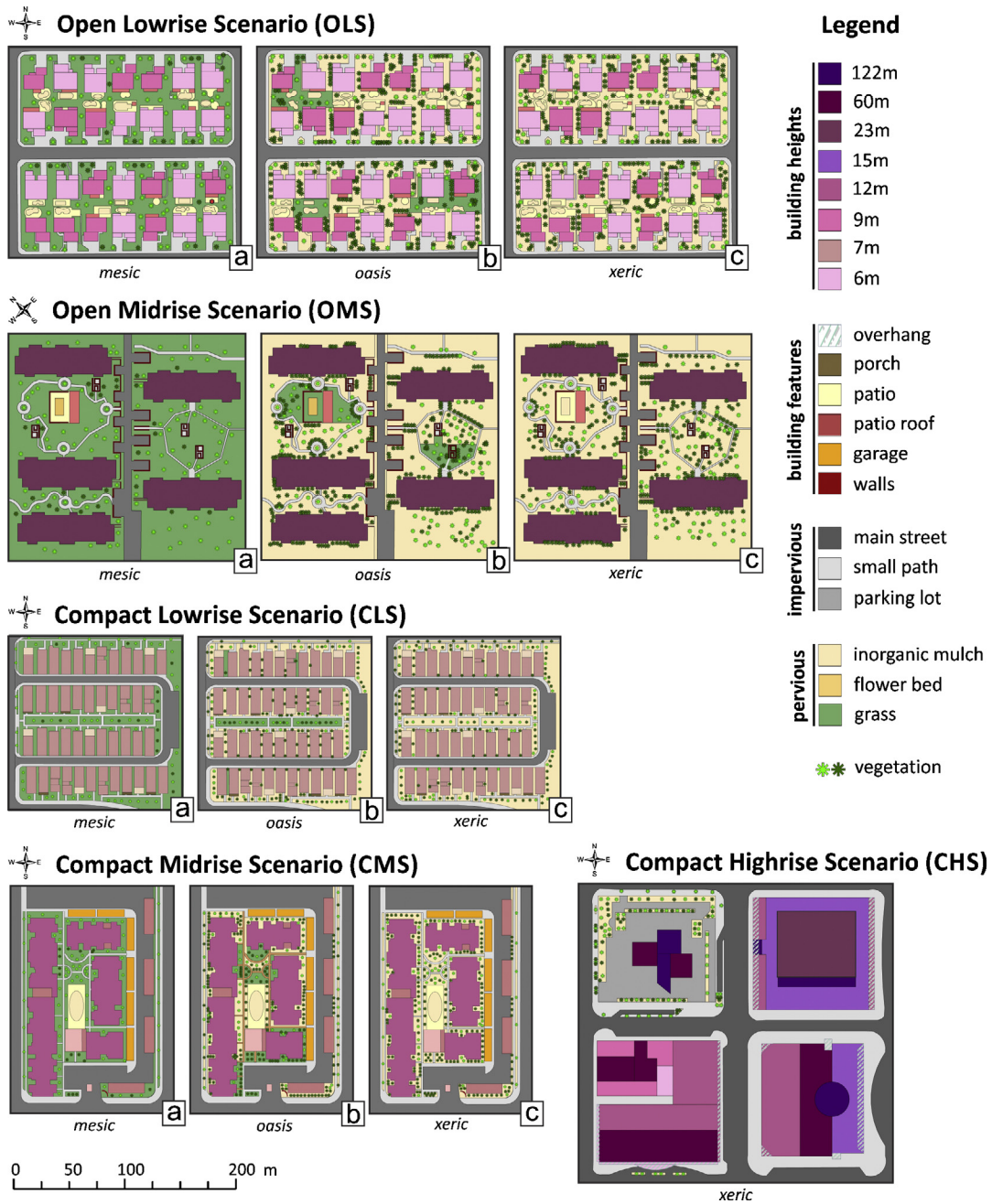
Fig. 6. Urban form scenarios classified into Local Climate Zones (LCZ) and combined with four landscaping options: (a) mesic, (b) oasis, (c) xeric.

stands out from all scenarios: Here, the mean standard deviation of T_{2m} is largest with a value of 0.7 °C.

As expected, the thermal hierarchy—xeric was always warmest followed by oasis then mesic—of the three landscaping scenarios was maintained for each urban form. A hierarchy could also be established for the LCZs. On average, the *Open Midrise* scenario is the warmest neighborhood, followed by *Compact Midrise*, *Open Lowrise*,

and *Compact Lowrise*. There was one exception—the mesic *Compact Midrise* scenario is slightly warmer than the mesic *Open Midrise* scenario, both in terms of daily averaged air temperatures and spatially averaged air temperatures at 15:00 h.

A very distinct temperature profile can be observed for the *Compact Highrise* scenario. Here, the diurnal temperature amplitude is smaller compared to other scenarios with warmer temperatures

Table 4

White columns: properties of select Local Climate Zones (Stewart & Oke, 2012); gray columns: properties of corresponding Phoenix neighborhoods selected for this study.

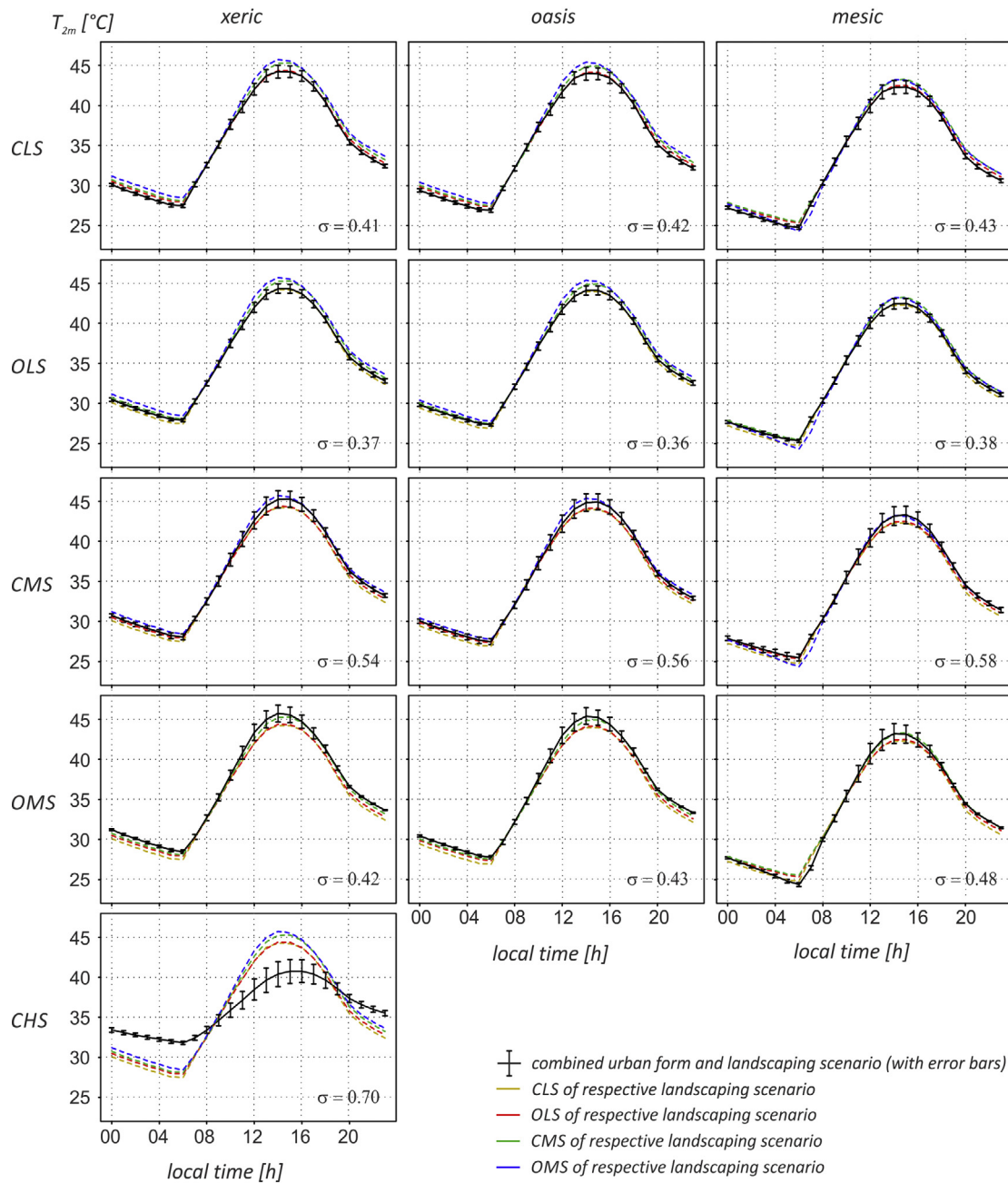|	Open low-rise		Open midrise		Compact low-rise		Compact midrise		Compact high-rise	
Sky view factor	0.6–0.9	0.6	0.5–0.8	0.5	0.2–0.6	0.6	0.3–0.6	0.5	0.2–0.4	0.4
Mean building height	3–10 m	7 m	10–25 m	23 m	3–10 m	7 m	10–25 m	10 m	>25 m	25 m
Building surface fraction	20–40%	30%	20–40%	26%	40–70%	40%	40–70%	39%	40–60%	47%
Impervious surface fraction	20–50%	29%	30–50%	12%	20–50%	27%	30–50%	52%	40–60%	48%
Surface Albedo	0.12–0.25	0.16	0.12–0.25	0.13	0.12–0.25	0.16	0.10–0.20	0.17	0.10–0.20	0.20

Fig. 7. Diurnal 2-m air temperature curve for each combined urban form and landscaping scenario, spatially averaged with error bars and averaged standard deviation σ. CHS = Compact Highrise Scenario, OMS = Open Midrise Scenario, OLS = Open Lowrise Scenario, CMS = Compact Midrise Scenario, CLS = Compact Lowrise Scenario.

during the night and early morning, but lower daytime temperatures. This effect is known as daytime cool island and has been reported by several authors. Chow and Roth (2006) discovered a daytime urban cool island for Singapore, and Erell and Williamson (2007) measured the daytime cool island for the city core of Adelaide, Australia under warm, clear and calm conditions. The authors explain this phenomenon through the central-urban building morphology: although high structures increase the overall surface to absorb and reflect direct solar radiation, the street level absorbs only a fraction of the direct solar energy due to increased shading. The simulation results for our *Compact Highrise* scenario are in line with these findings.

To further investigate thermal differences between the scenarios at the time of the daily maximum, we created a histogram for the relative frequency of 2-m air temperature values in the model area at 15:00 h (Fig. 8). The temperature range in the midrise scenarios

is larger than in the corresponding lowrise scenarios. It is largest for the *Compact Highrise* scenario, which, at the same time, is the coolest neighborhood in mid-afternoon. The validation scenarios included in the histogram are more sparsely built than their *Open Lowrise* scenario counterparts and exhibit higher temperatures. Similarly, the open scenarios feature higher temperatures than the compact scenarios in nearly all cases, indicating that extensive open areas contribute to higher daytime temperatures due to a lack of shading.

3.2. Spatial distribution of near-ground air temperatures and airflow

Fig. 9 demonstrates the findings outlined in this section. These include the near-ground air temperatures for 15:00 h, which were mapped for each scenario using the LEONARDO tool included in
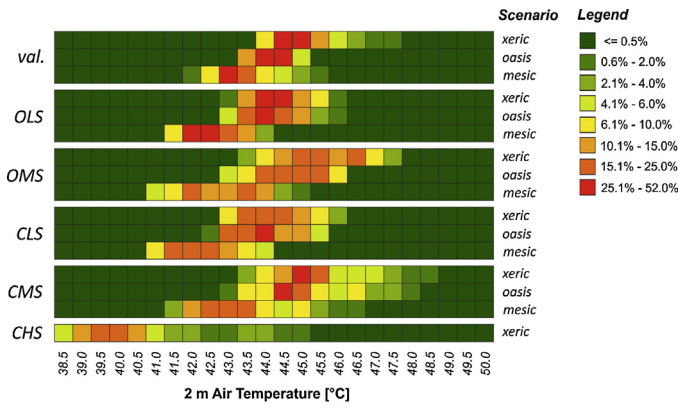
Fig. 8. Histogram for 2-m air temperature distribution: For each scenario (rows), the occurrence of temperatures (rounded to 0.5 °C) in percent (columns) is mapped (val. = validation run, OLS = Open Lowrise Scenario, OMS = Open Midrise Scenario, CLS = Compact Lowrise Scenario, CMS = Compact Midrise Scenario, CHS = Compact Highrise Scenario).

the ENVI-met package. In general, within-scenario air temperature patterns are similar to each other across landscaping scenarios, with a hierarchy from cool (mesic) to warm (xeric), but patterns vary across LCZs. The distribution of air temperatures follows the wind direction, with higher temperatures at the west side of the neighborhoods and lower temperatures at the east side. This can be observed in each LCZ, but is very pronounced in the two midrise scenarios. Higher temperatures at the west border of the study sites are an artifact of the model's boundary conditions. Within the neighborhoods, lower temperatures on the lee-side of buildings compared to their windward-side are due to shading and small advective effects. In the *Compact Midrise* scenarios, the apartment building to the west shields high mid-afternoon temperatures from the central courtyard, lowering air temperatures in the courtyard by about 2 °C for each landscape design (Fig. 9). This relatively large within-design temperature difference is also reflected in the high standard deviation, as shown previously in Fig. 7. A similar trend can be observed for the *Open Midrise* scenarios. Since this LCZ features more open space, air temperatures are less variable, although areas with high temperatures are more extended. Thermal differences around the apartment to the east are not as significant as differences around other structures in the study area, which is, again, due to the shading effect of the apartments to the west.

The air temperature maximum at 15:00 h occurs at the east border of the model area in all midrise and lowrise scenarios, except the *Compact Highrise* scenario, which shows a different pattern. Here, the area with the highest air temperatures is located at the southwest corner of the model domain. The buildings to the west are not shaded, because they are located at the border of the study area and are subject to ENVI-met's boundary conditions. In contrast, the northeast corner of the model area is coolest, and it also exhibits relatively low surface temperatures. The cooling effect of the highrise building can also be observed in the diurnal air temperature profile. A cool patch near the highrise structure moves around the building during the day, following the course of the shade. A video showing the hourly diurnal development of air temperatures is provided in the supplementary material of this article.

In the *Compact Lowrise* scenario, averaged 15:00 h air temperatures at 2-m are 0.2–0.3 °C lower than in the *Open Lowrise* scenario. Although both spatial plots reveal a similar temperature distribution, the air temperature between buildings is generally lower in the *Compact Lowrise* scenario. Compared to the *Open Lowrise* scenario, modeled wind speed between buildings is also lower in the compact setting, revealing a less significant advective effect and locally allowing for other processes such as shading to dominate the thermal situation.

In contrast, the open spaces between building rows behave similarly in both LCZs. We hypothesize that these east–west street canyons function as air channels, accelerating the wind. Therefore, a wider channel in the center of each scenario, parallel to the wind direction, facilitates lower daytime temperatures at the windward-side regardless of surface materials. In the evening though, air temperatures above pervious surfaces exceed those above impervious surfaces. These modeling results need to be confirmed through actual measurements in a subsequent study. Again, a video in the supplementary material illustrates the diurnal 2-m air temperature progression for the xeric scenarios.

In dense urban forms, compact street canyons can create a potential "cool island" through internal shading effects (Pearlmutter et al., 2009). The cooling effect of local shading patterns becomes particularly evident when comparing surface temperatures and incoming direct shortwave radiation in our *Compact Highrise* scenario (Fig. 10). To analyze the impact of urban form and fabric on surface temperatures, we ran a multiple regression analysis with surface temperatures as dependent variable and surface materials and shading as independent variables.

The four-category surface materials factor is represented by a set of three dummy regressors (0/1): Mohall loam with inorganic mulch, asphalt, and concrete. The omitted category, "other" surface materials, is coded 0 for all dummy variables in the set and serves as baseline category. Incoming direct shortwave radiation was entered into the regression as an indicator variable for shade, coded "1" if incoming solar < maximum value (grid is partly in the shade) or incoming solar = 0 (grid is fully shaded) and "0" if incoming solar = maximum value (no shade). Table 5 summarizes the number of cases for each dummy variable with mean surface temperature and standard deviation. Overall, Mohall loam covered with inorganic mulch is the coolest of all surface materials (51.27 ± 3.26 °C) and asphalt the hottest (64.29 ± 5.71 °C). Shaded surfaces are, on average, 11 °C cooler than exposed surfaces.

Our multiple regression model for $n = 12{,}934$ grids in the *Compact Highrise* scenario with four predictors (three surface material dummy variables and a dichotomous shade factor) is statistically significant with an *F*-test *p*-value of zero to three decimal places. All independent variables are significant (0.000) at the 0.05 alpha level. Pearson's correlations between each predictor variable and the surface temperature at 15:00 h are $r = -.728$ (shade), $r = -.359$ (Mohall loam with inorganic mulch), $r = .404$ (asphalt), and $r = -.256$ (concrete). The adjusted coefficient of multiple determination is $R^2 = 0.712$, showing that 71.2% of the surface temperature variability is explained by the model and that our independent variables reliably predict surface temperatures at 15:00 h. Concluding from the standardized partial regression coefficients β, shade is the strongest predictor of surface temperatures and has a cooling effect ($\beta = -.691$), followed by Mohall loam with inorganic mulch ($\beta = -.352$) and concrete ($\beta = -.093$). Asphalt ($\beta = -.145$) has a warming effect due to its high volumetric heat capacity.

4. Discussion

We systematically analyzed how various urban form and landscaping designs impact urban heating and cooling to better understand microclimatic dynamics in semi-arid environments. In this study, cooling is only reflected by air temperature and surface temperature differences, not by an integrated representation of microclimatic effects on a pedestrian. Such thermal comfort considerations would have to include an analysis of radiation and wind effects on the human body (e.g., Pearlmutter, Berliner, & Shaviv, 2007a) and will be part of future work.

The results of this study confirm prior efforts that found substantial air temperature cooling benefits from vegetation
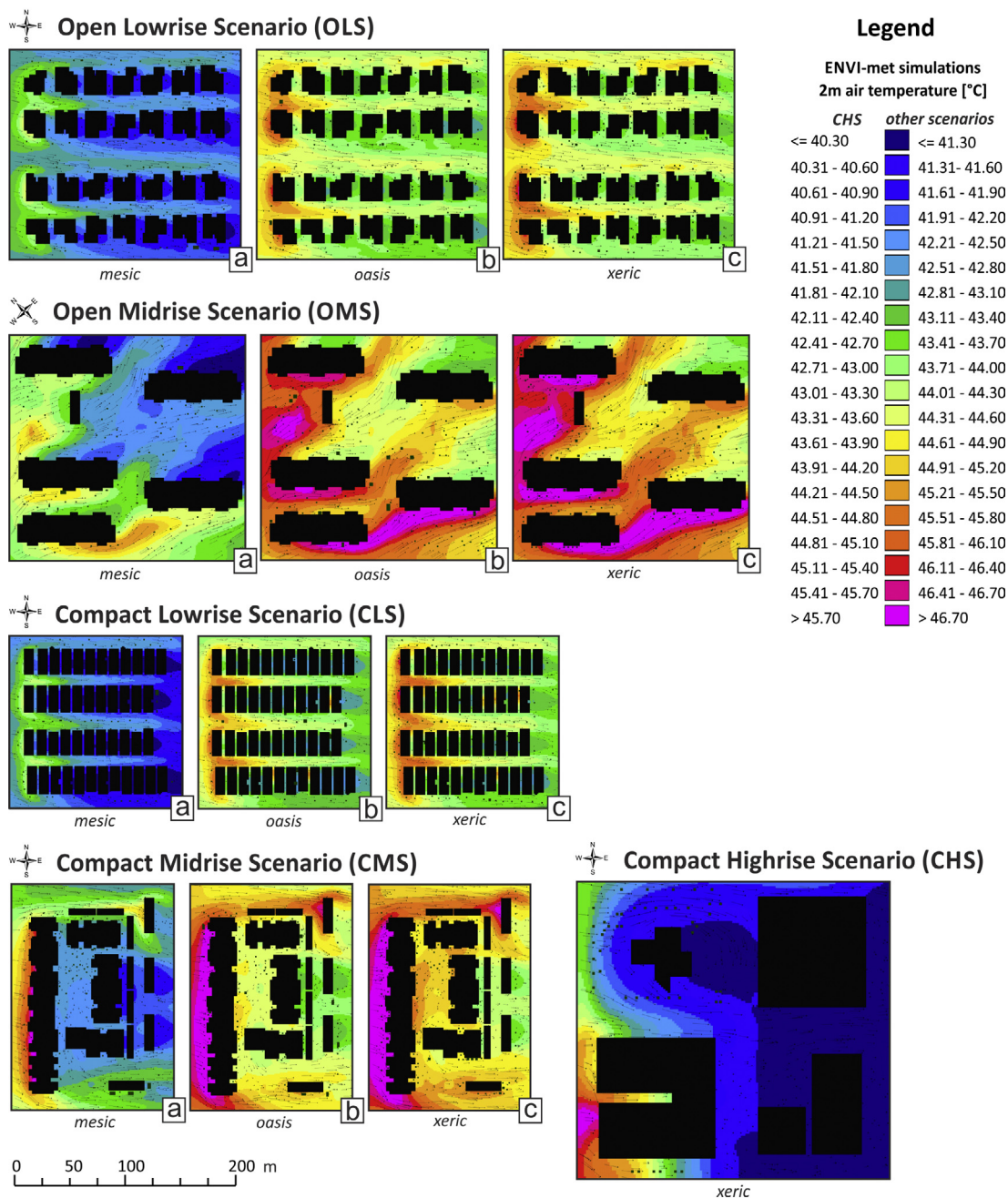
Open Lowrise Scenario (OLS)

mesic a   oasis b   xeric c

Open Midrise Scenario (OMS)

mesic a   oasis b   xeric c

Compact Lowrise Scenario (CLS)

mesic a   oasis b   xeric c

Compact Midrise Scenario (CMS)

mesic a   oasis b   xeric c

0 50 100 200 m

Compact Highrise Scenario (CHS)

xeric

Legend

ENVI-met simulations
2m air temperature [°C]

CHS	other scenarios
<= 40.30	<= 41.30
40.31 - 40.60	41.31- 41.60
40.61 - 40.90	41.61 - 41.90
40.91 - 41.20	41.91 - 42.20
41.21 - 41.50	42.21 - 42.50
41.51 - 41.80	42.51 - 42.80
41.81 - 42.10	42.81 - 43.10
42.11 - 42.40	43.11 - 43.40
42.41 - 42.70	43.41 - 43.70
42.71 - 43.00	43.71 - 44.00
43.01 - 43.30	44.01 - 44.30
43.31 - 43.60	44.31 - 44.60
43.61 - 43.90	44.61 - 44.90
43.91 - 44.20	44.91 - 45.20
44.21 - 44.50	45.21 - 45.50
44.51 - 44.80	45.51 - 45.80
44.81 - 45.10	45.81 - 46.10
45.11 - 45.40	46.11 - 46.40
45.41 - 45.70	46.41 - 46.70
> 45.70	> 46.70

Fig. 9. Snapshots of the air temperature distribution at 2 m height for each combined urban form and landscaping scenario for June 23, 2011, 15:00 h.

(Guhathakurta & Gober, 2010; Middel, Brazel, Gober, et al., 2012; Middel, Brazel, Kaplan, et al., 2012). Mesic sites were found to be the coolest landscapes, followed by oasis then xeric. Results further show that cooling is not only a function of vegetation and surface materials, but also dependent on the form and spatial arrangement

of urban features. In terms of urban form, compact scenarios were most advantageous for daytime cooling. Our findings suggest that, at the microscale, urban form has a larger impact on daytime temperatures than landscaping. In addition, our findings indicate that small patches of grass in the oasis type of landscapes do

Table 5
Descriptive statistics.

Category	Number of cases	Mean surface temperature [°C]	Standard deviation
Mohall loam with inorganic mulch	653	51.27	±3.26
Asphalt	6150	64.29	±5.71
Pavement (concrete)	4483	59.19	±5.88
Other surface materials	1648	61.46	±5.85
Shade	3156	53.08	±4.79
No shade	9778	64.22	±4.42
All grids	12,934	61.51	±6.57

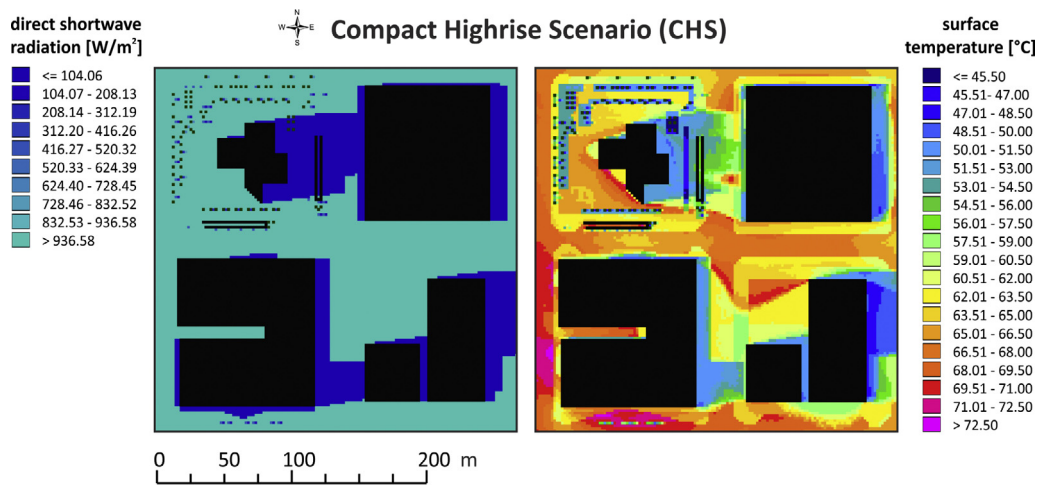**Fig. 10.** Direct shortwave radiation [W m^{-2}] and surface temperatures [°C] at 15:00 h for the *Compact Highrise* scenario.

not result in a significant daytime cooling benefit compared to compact urban forms. We hypothesize that effective daytime cooling is noticeable only after a threshold of vegetation density is reached. More research is necessary to find the appropriate balance between water intensive vegetation and energy savings from its cooling impact.

The current version of the ENVI-met model does not simulate a diurnal cycle for wind or wind direction changes, which would be critical to evaluate for a place with thermal slope valley wind systems such as Phoenix on a diurnal basis. Therefore, the application of ENVI-met in our study area was limited to a certain point in time (15:00 h) and involved an extensive validation effort. Furthermore, each scenario run was analyzed in isolation and advection or shading effects between neighborhoods could not be taken into account. Despite these limitations, ENVI-met adequately captured mid-afternoon microscale dynamics in typical Phoenix area neighborhoods. Future work will include a comparison of our results to nighttime microclimate in Phoenix LCZs, as we suspect that the most effective urban forms for daytime cooling may not be beneficial at night due to the capacity of the urban fabric to store and trap heat. This future work will provide insight into how sustainable urban designs can incorporate balanced cooling benefits for daytime and nighttime situations.

The overall scale of the ENVI-met model and approach fits well with the concept of LCZs, which were developed from universally recognized urban forms and land cover (Stewart & Oke, 2012). Therefore, the LCZ classification scheme not only is a comprehensive framework for UHI research, it is also a useful concept for integrating local climate knowledge into urban planning and design practices.

5. Conclusion

The goal of this study was to find planning and urban design solutions for reducing excessive heat in urban neighborhoods. The most significant conclusion that we can draw from our results addresses the ongoing debate about the virtues of compact development. While compact development has many benefits from, e.g., transportation energy savings, prior studies have also noted that high concentrations of buildings, structures, and impervious surfaces increase radiative heating and intensify UHI effects. While our study does not speak to the factors affecting nighttime temperatures, it does show that the daytime shading properties of tall buildings play a significant role in reducing urban heat. The results also indicate that urban canyon effects produced by arrangement

of mid- to high-rise buildings along the direction of wind flow help in reducing daytime temperatures.

Thus, we conclude that sustainable urban development does not only entail smart growth (i.e., compact growth) but also smart design. Appropriate design solutions are critical for realizing the benefits of smart growth, and our study showed that the LCZ concept combined with ENVI-met is a powerful planning tool to identify and develop sustainable urban forms and landscapes that ameliorate temperatures in desert cities through smart design.

Acknowledgements

Appendix A. Supplementary data

Supplementary data associated with this article can be found, in the online version, at http://dx.doi.org/10.1016/j.landurbplan.2013.11.004.

References

Adams, E. D. (1974). *Soil survey of eastern Maricopa and northern Pinal Counties area, Arizona*. Washington, DC: U.S. Government Printing Office.

Arnfield, A. J. (2003). Two decades of urban climate research: A review of turbulence, exchanges of energy and water, and the urban heat island. *International Journal of Climatology*, 23(1), 1–26. http://dx.doi.org/10.1002/joc.859

Balling, R. C., & Cerveny, R. S. (1987). Long-term association between wind speeds and the urban heat island of Phoenix, Arizona. *Journal of Climate and Applied Meteorology*, 20(6), 712–716. http://dx.doi.org/10.1175/1520-0450(1987)026%3C0712:LTABWS%3E2.0.CO;2

Bonan, G. B. (2000). The microclimates of a suburban Colorado (USA) landscape and implications for planning and design. *Landscape and Urban Planning*, 49(3), 97–114. http://dx.doi.org/10.1016/S0169-2046(00)00071-2

Brazel, A. J., Selover, N., Vose, R., & Heisler, G. (2000). The tale of two cities: Baltimore and Phoenix urban LTERs. *Climate Research*, 15(2), 123–135. http://dx.doi.org/10.3354/cr015123

Bruse, M. (2004). *ENVI-met 3.0: Updated Model Overview.* Retrieved from http://www.envi-met.com/documents/papers/overview30.pdf

Bruse, M. (2013). *ENVI-met 3.1 BETA V.* Retrieved from http://www.envi-met.com/

Chow, W. T. L., & Brazel, A. J. (2011). Assessing xeriscaping as a sustainable heat island mitigation approach for a desert city. *Building and Environment*, 47(1), 170–181. http://dx.doi.org/10.1016/j.buildenv.2011.07.027

Chow, W. T. L., Pope, R. L., Martin, C. A., & Brazel, A. J. (2011). Observing and modeling the nocturnal park cool island of an arid city: Horizontal and vertical impacts. *Theoretical and Applied Climatology*, 103(1–2), 197–211. http://dx.doi.org/10.1007/s00704-010-0293-8

Chow, W. T. L, & Roth, M. (2006). Temporal dynamics of the urban heat island of Singapore. *International Journal of Climatology*, 26(15), 2243–2260. http://dx.doi.org/10.1002/joc.1364

Ellis, A. W., Hildebrandt, M. L., Thomas, W. M., & Fernando, H. J. S. (2000). Analysis of the climatic mechanisms contributing to the summertime transport of lower atmospheric ozone across metropolitan Phoenix, Arizona, USA. *Climate Research*, 15(1), 13–31. http://dx.doi.org/10.3354/cr015013

Emmanuel, R., & Fernando, H. J. S. (2007). Urban heat islands in humid and arid climates: Role of urban form and thermal properties in Colombo, Sri Lanka and Phoenix, USA. *Climate Research*, 34(3), 241–251. http://dx.doi.org/10.3354/cr00694

Erell, E., & Williamson, T. (2007). Intra-urban differences in canopy layer air temperature at a mid-latitude city. *International Journal of Climatology*, 27(9), 1243–1255. http://dx.doi.org/10.1002/joc.1469

Fraunhofer IRB. (2012). (*Material data collection for energetic retrofitting of old buildings*) *Materialdatensammlung für die energetische Altbausanierung.* Retrieved from http://www.irb.fraunhofer.de/denkmalpflege/angebote_partner/masea/

Georgescu, M., Moustaoui, M., Mahalov, A., & Dudhia, J. (2011). An alternative explanation of the semiarid urban area "oasis effect". *Journal of Geophysical Research*, 116(D24), 1–13. http://dx.doi.org/10.1029/2011JD016720

Gober, P., Middel, A., Brazel, A. J., Myint, S. W., Chang, H., Duh, J.-D., et al. (2012). Tradeoffs between water conservation and temperature amelioration in Phoenix and Portland: Implications for urban sustainability. *Urban Geography*, 33(7), 1030–1054. http://dx.doi.org/10.2747/0272-3638.33.7.1030

Golden, J. S. (2004). The built environment induced urban heat island effect in rapidly urbanizing arid regions – A sustainable urban engineering complexity. *Journal of Integrative Environmental Sciences*, 1(4), 321–349. http://dx.doi.org/10.1080/15693430412331291698$16.00

Guhathakurta, S., & Gober, P. (2007). The impact of the Phoenix urban heat island on residential water use. *Journal of the American Planning Association*, 73(3), 317–329. http://dx.doi.org/10.1080/01944360708977980

Guhathakurta, S., & Gober, P. (2010). Residential land use, the urban heat island, and water use in Phoenix: A path analysis. *Journal of Planning Education and Research*, 30(1), 40–51. http://dx.doi.org/10.1177/0739456X10374187

Harlan, S., Brazel, A. J., Prashad, L., Stefanov, W. L., & Larsen, L. (2006). Neighborhood microclimates and vulnerability to heat stress. *Social Science & Medicine*, 63(11), 2847–2863. http://dx.doi.org/10.1016/j.socscimed.2006.07.030

Hart, M. A., & Sailor, D. J. (2009). Quantifying the influence of land-use and surface characteristics on spatial variability in the urban heat island. *Theoretical and Applied Climatology*, 95(3–4), 397–406. http://dx.doi.org/10.1007/s00704-008-0017-5

Jenerette, G. D., Middel, A., Harlan, S. L., Stefanov, W. L., & Martin, C. L. (2011). Ecosystem services and urban heat riskscape moderation: Water, green spaces, and social inequality in Phoenix, USA. *Ecological Applications*, 21(7), 2637–2651. http://dx.doi.org/10.1890/10-1493.1

Jenkins, J. C., Chojnacky, D. C., Heath, L. S., & Birdsey, R. A. (2004). *Comprehensive database of diameter-based biomass regressions for North American tree species, Research Paper NE-319* p. 45. Newtown Square, PA: U.S. Department of Agriculture, Forest Service, Northeastern Research Station.

Lalic, B., & Mihailovic, D. T. (2004). An empirical relation describing leaf-area density inside the forest for environmental modeling. *Journal of Applied Meteorology and Climatology*, 43(4), 641–645. http://dx.doi.org/10.1175/1520-0450(2004)043<0641:AERDLD>2.0.CO;2

Martin, C. A., Busse, K., & Yabiku, S. (2007). North Desert Village: The effect of landscape manipulation on microclimate and its relation to human landscape preferences. *HortScience*, 42(4), 853–854.

MesoWest. (2012). *MesoWest Data.* University of Utah. Retrieved from http://mesowest.utah.edu/index.html

Middel, A., Brazel, A. J., Gober, P., Myint, S. W., Chang, H., & Duh, J.-D. (2012). Land cover, climate, and the summer surface energy balance in Phoenix, AZ and Portland, OR. *International Journal of Climatology*, 32(13), 2020–2032. http://dx.doi.org/10.1002/joc.2408

Middel, A., Brazel, A. J., Kaplan, S., & Myint, S. W. (2012). Daytime cooling efficiency and diurnal energy balance in Phoenix, AZ. *Climate Research*, 54(1), 21–34. http://dx.doi.org/10.3354/cr01103

NRCS. (2012). *Natural Resources Conservation Service.* Retrieved from http://websoilsurvey.nrcs.usda.gov/

Pearlmutter, D., Berliner, P., & Shaviv, E. (2007a). Integrated modeling of pedestrian energy exchange and thermal comfort in urban street canyons. *Building and Environment*, 42(6), 2396–2409. http://dx.doi.org/10.1016/j.buildenv.2006.06.006

Pearlmutter, D., Berliner, P., & Shaviv, E. (2007b). Urban climatology in arid regions: Current research in the Negev desert. *International Journal of Climatology*, 27(14), 1875–1885. http://dx.doi.org/10.1002/joc.1523

Pearlmutter, D., Bitan, A., & Berliner, P. (1999). Microclimatic analysis of "compact" urban canyons in an arid zone. *Atmospheric Environment*, 33(24–25), 4143–4150. http://dx.doi.org/10.1016/S1352-2310(99)00156-9

Pearlmutter, D., Krüger, E. L., & Berliner, P. (2009). The role of evaporation in the energy balance of an open-air scaled urban surface. *International Journal of Climatology*, 29(6), 911–920. http://dx.doi.org/10.1002/joc.1752

Sarrat, C., Lemonsu, A., Masson, V., & Guedalia, D. (2006). Impact of urban heat island on regional atmospheric pollution. *Atmospheric Environment*, 40(10), 1743–1758. http://dx.doi.org/10.1016/j.atmosenv.2005.11.037

Schenk, H. J., & Jackson, R. B. (2002). Rooting depths, lateral root spreads and below-ground/above-ground allometries of plants in water-limited ecosystems. *Journal of Ecology*, 90(3), 480–494. http://dx.doi.org/10.1046/j.1365-2745.2002.00682.x

Shashua-Bar, L., Pearlmutter, D., & Erell, E. (2009). The cooling efficiency of urban landscape strategies in a hot dry climate. *Landscape and Urban Planning*, 92(3–4), 179–186. http://dx.doi.org/10.1016/j.landurbplan.2009.04.005

Singer, C. K., & Martin, C. A. (2008). Effect of landscape mulches on desert landscape microclimates. *Arboriculture and Urban Forestry*, 34(4), 230–237.

Stewart, I. D., & Oke, T. R. (2012). Local climate zones for urban temperature studies. *Bulletin of the American Meteorological Society*, 93(12), 1879–1900. http://dx.doi.org/10.1175/BAMS-D-11-00019.1

Stone, B., & Norman, J. M. (2006). Land use planning and surface heat island formation: A parcel-based radiation flux approach. *Atmospheric Environment*, 40, 3561–3573. http://dx.doi.org/10.1016/j.atmosenv.2006.01.015

University of Wyoming. (2012). *Atmospheric Soundings.* Retrieved from http://weather.uwyo.edu/upperair/sounding.html

Willmott, C. J. (1981). On the validation of models. *Physical Geography*, 2, 184–194.

Willmott, C. J. (1982). Some comments on the evaluation of model performance. *Bulletin of the American Meteorological Society*, 63(11), 1309–1313.